ELSEVIER

Available online at www.sciencedirect.com
SCIENCE DIRECT

Journal of Crystal Growth 267 (2004) 35–41

JOURNAL OF CRYSTAL GROWTH

www.elsevier.com/locate/jcrysgro

Low-resistance n-type polycrystalline InAs grown by molecular beam epitaxy

Dennis W. Scott*, Christoph Kadow, Yingda Dong, Yun Wei, Arthur C. Gossard, Mark J.W. Rodwell

Department of Electrical and Computer Engineering, University of California, 5152 Engineering I, Santa Barbara, CA 93106, USA

Received 14 February 2004; accepted 18 March 2004
Communicated by D.W. Shaw

Abstract

We report growth and electrical properties of low-resistance, silicon-doped polycrystalline InAs (poly-InAs) by molecular beam epitaxy. The material was characterized by Hall measurements, scanning electron microscopy, and transmission line measurements. The resistivity of poly-InAs is found to have a strong dependence on film thickness and grain size as well as the density of the crystallite grains. The low-resistivity poly-InAs is proposed as an extrinsic emitter contact material in III–V heterojunction bipolar transistors similar to the polycrystalline silicon used as contacts in silicon bipolar junction transistor technology.
© 2004 Elsevier B.V. All rights reserved.

PACS: 81.15.H

Keywords: A3. Molecular beam epitaxy; B1. Arsenides; B2. Semiconducting III–V materials; B3. Bipolar transistor

1. Introduction

Ion implanted polycrystalline silicon (polysilicon) is an important material in the fabrication of silicon bipolar junction transistors (BJTs) and SiGe heterojunction bipolar transistors (HBTs). Polysilicon contacts to the extrinsic base placed over dielectric spacer layers have been successfully employed to reduce base-collector capacitance [1], while polysilicon emitter contacts are used as both the contact and diffusion source in self-aligned bipolar transistors [2,3]. There has been a recent trend in SiGe HBTs towards 100 nm emitter widths [4–6]. As emitter widths move towards 100 nm, some attention has been given to the optimization of the extrinsic polycrystalline electrode to reduce resistance in the narrow emitter contact [7].

As the emitter dimensions of III–V HBTs also scale towards deep sub-micron dimensions, a similar emitter contact method may be applied to create an extrinsic emitter contact wider than the base–emitter junction width [8,9], thereby reducing emitter access resistance. As shown in Fig. 1, a low-resistance polycrystalline material may be employed as an extrinsic emitter contact layer

*Corresponding author. Tel.: +1-805-893-8044; fax: +1-805-893-3262.
E-mail address: dennis@umail.ucsb.edu (D.W. Scott).

0022-0248/$ - see front matter © 2004 Elsevier B.V. All rights reserved.
doi:10.1016/j.jcrysgro.2004.03.049

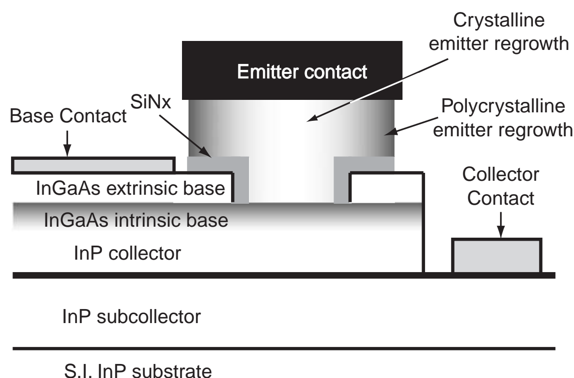

Fig. 1. Proposed III–V HBT with extrinsic emitter contact layer over a buried dielectric.

over a buried dielectric in a regrown emitter HBT. Using this structure, the emitter contact area and resistance may be preserved as emitter junction regions are scaled towards deep sub-micron dimensions. Although papers have also been presented using selective emitter regrowth [10,11] where minimal extrinsic emitter area is formed, a wide extrinsic emitter contact formed by non-selective emitter regrowth may prove beneficial as base–emitter junction areas are further scaled.

This report details a study where n-type InAs has been chosen as a potential candidate for the polycrystalline extrinsic emitter material. This choice is motivated by the narrow bandgap and, therefore, high carrier mobility of monocrystalline InAs bulk material. InAs also has a favorable Fermi-level pinning in the conduction band [12,13]. This avoids carrier depletion through Fermi-level pinning at grain boundaries, an effect that would increase resistivity. In this work, we study the electrical characteristics of low-resistance, silicon-doped polycrystalline InAs (poly-InAs) deposited by non-selective molecular beam epitaxy (MBE). We examine several aspects of the growth conditions and their effect on the conductive properties of the film.

2. Experimental procedures

Poly-InAs samples were deposited in a solid-source Varian Gen II MBE system equipped with a valved arsenic source. The n-type dopant was silicon. The poly-InAs samples were grown on 2-in, semi-insulating (1 0 0) GaAs substrates coated with SiN_x. Prior to SiN_x deposition, the GaAs wafers were cleaned with solvent and thoroughly rinsed in deionized water. The native oxide was then removed using a dilute HF solution followed by a thorough rinse in deionized water. A 1500 Å SiN_x film was deposited by plasma-enhanced chemical vapor deposition (PECVD) onto the GaAs wafers at a temperature of 300°C. The SiN_x was then lithographically patterned, and a 1 cm square area of dielectric was removed from the center of each wafer using HF etchant. This area of exposed GaAs allows for consistent temperature monitoring by pyrometer and for observation of the RHEED signal while in the MBE system.

The coated GaAs wafers were heated in the MBE growth chamber under an arsenic over-pressure to a substrate temperature of over 600°C, and oxide desorption was confirmed by RHEED in the exposed GaAs regions. The substrate temperature was then lowered for InAs deposition. The InAs growths were performed at various temperatures ranging from 430°C to 490°C. The arsenic to indium (V–III) ratios were varied from 10 to 40 according to beam equivalent pressure (BEP) measurements. Deposition thicknesses were varied from about 750 to 3200 Å. These thicknesses were initially estimated for growth using monocrystalline InAs growth rates determined by RHEED. Measurements of the actual maximum thickness for each of the poly-InAs samples were then determined by ex situ height profilometry. The maximum thickness measurements were also confirmed by SEM cross-section on the samples of varied thickness. Growth rates for the poly-InAs depositions were maintained at about 0.36 μm/h. This growth rate was initially estimated from monocrystalline InAs RHEED and corrected by ex situ maximum height measurements. A fixed silicon doping cell temperature was used for all of the poly-InAs growths. This particular silicon cell temperature corresponds to a $1 \times 10^{19}\,cm^{-3}$ doping level in InP lattice-matched InGaAs grown at a rate of 1.0 μm/h. No attempts were made during this study to optimize the doping level for maximum conductivity in poly-InAs.

Room temperature Hall measurements were used to determine sheet concentration and mobility for each of the growths. Indium contacts were formed on the van der Pauw samples and annealed for less than 3 min at a temperature of 150°C. Each sample was then patterned and etched to determine the maximum poly-InAs thicknesses by height profilometry. Plan-view SEM images were used to determine the grain size variation in all samples. TLM patterns with Ti/Pt/Au contacts were fabricated for most samples to confirming the Hall data. The TLM measurements were also used to demonstrate that the low contact resistivity of poly-InAs is preserved. Contact resistivities range from 0.5 to 80 $\Omega\,\mu m^2$ [9,14].

3. Results and discussion

Four approximately 1300 Å thick poly-InAs samples were grown at different temperatures while maintaining a fixed V–III ratio of 20. The growth temperatures were varied from 430°C to 490°C in 20°C increments. Fig. 2(a) shows the dependence of each sample's electron concentration and mobility on growth temperature. A highly non-uniform surface morphology is observed by macroscopic inspection of the 490°C growth sample. After several attempts to improve the growth at 490°C, we conclude that the temperature is too high to maintain uniform deposition onto the SiN_x templates. The non-uniformity may be due to poor nucleation and/or adhesion onto SiN_x at this temperature. It is noted, however, that the deposition of InAs in the exposed GaAs window is uniform at all growth temperatures including the 490°C sample.

The degradation of growth at 490°C is also evident in the electrical properties for that sample. For growths between 430°C and 470°C we observe a strong dependence of the electron mobility on growth temperature and a weaker effect on the electron concentration. The increased mobility may be attributed to grain size dependence at the various temperatures. Fig. 3 shows plan-view SEM images for all growth temperatures. There is a clear trend towards larger grain size with higher growth temperature. However, there also appears

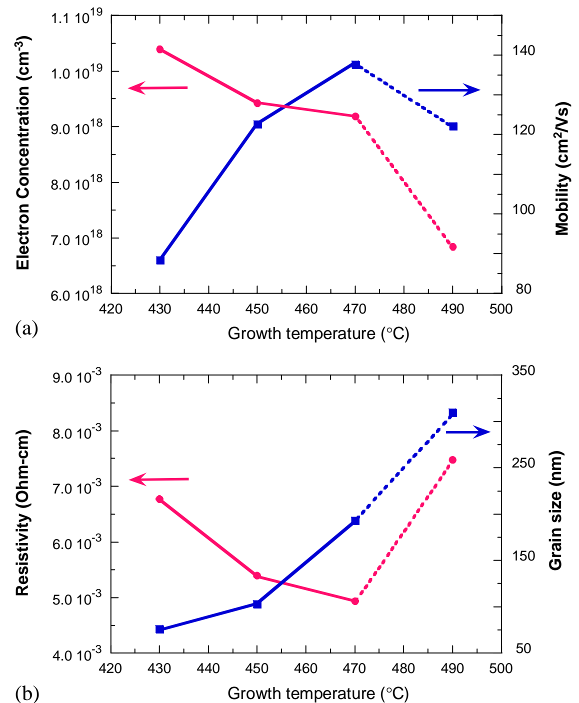

Fig. 2. Dependence of poly-InAs sample (a) electron concentration and mobility, and (b) resistivity and grain size on growth temperature.

to be a reduction in the density of the crystallites at higher temperatures. The grain density for the 490°C growth is especially degraded, and we believe this may account for the degradation in mobility despite the large grain size. Fig. 2(b) shows the grain size and resistivity for all samples versus growth temperature. Grain size becomes larger with higher growth temperature, ranging from an average of about 75 nm at 430°C to an average of about 310 nm for the 490°C growths. For samples grown at temperatures less than 490°C, there is a clear trend of resistivity decreasing with increased grain size.

The second set of poly-InAs samples was grown at varying arsenic to indium beam flux ratios ranging from 10 to 40 while maintaining a fixed growth temperature of 470°C. Fig. 4 shows the electron concentration and mobility of these samples as a function of V–III ratio. An arsenic to indium ratio of 10 gives poor carrier characteristics that do not follow the trends of the higher

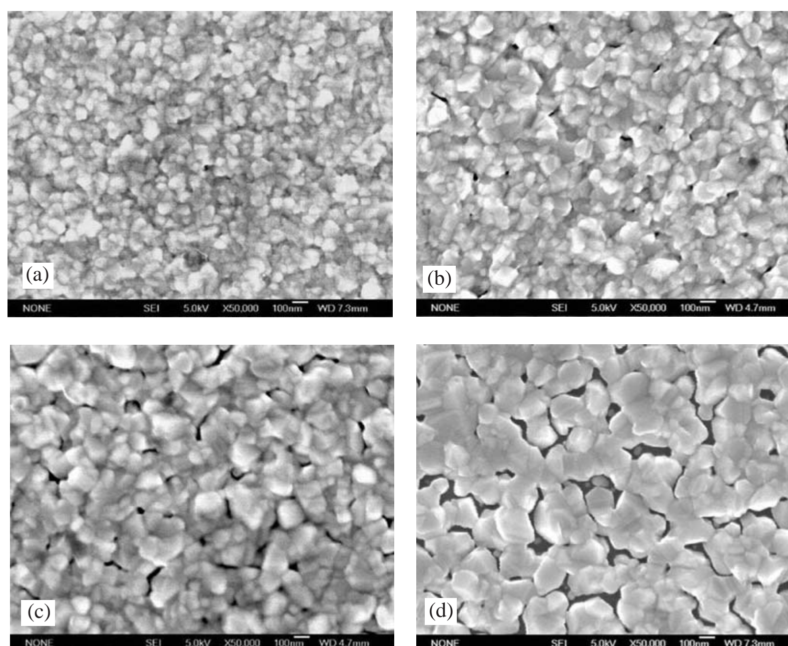

Fig. 3. Plan-view SEM images of poly-InAs samples grown at temperatures (a) 430°C, (b) 450°C, (c) 470°C, and (d) 490°C.

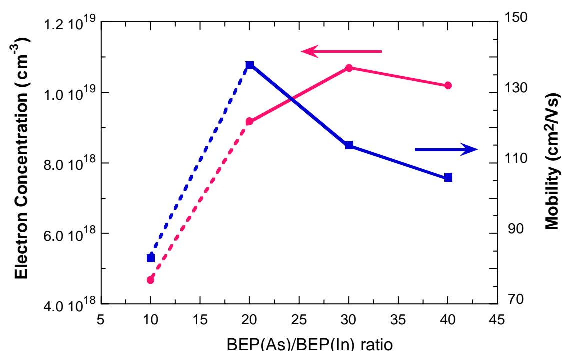

Fig. 4. Dependence of electron concentration and mobility of poly-InAs samples on V–III ratio.

V–III ratios. We believe this poor response to be indicative of an As-poor growth region for deposition onto SiN_x. In the remaining samples the electron mobility shows a strong decreasing trend with increased V–III ratio. A study of InAs growth on GaAs by MBE has shown that growth carried out under conditions leading to In-stable reconstruction results in higher quality bulk InAs material [15,16]. This finding suggests that lower arsenic to indium ratio will produce InAs crystallites that are closer to stoichiometric, and this accounts for the higher mobility at lower V–III ratios. In this set of samples, it is found that the change in V–III ratio does not significantly affect the electron concentration. The dependence of grain size on V–III ratio is also weak.

The third set of poly-InAs samples was grown with maximum film thickness varying from 750 to 3200 Å at a growth temperature of 470°C. Fig. 5(a) shows the variation in resistivity and grain size as a function of film thickness. The resistivity of the poly-InAs has a strong dependence on the maximum film thickness with lower resistivity at higher thicknesses. Moreover, the sheet resistivity is not proportional to the reciprocal of film thickness as in monocrystalline material over the *entire* thickness range studied in this report. Instead, the resistivity decreases very rapidly as the thickness approaches 1300 Å. The resistivity then follows a strong but less aggressive dependence as thickness increases, and this dependence appears to approach a constant linear relationship as expected in monocrystalline material. Fig. 5(b) shows that the electron concentration is also not weakly dependent on the film thickness. However,

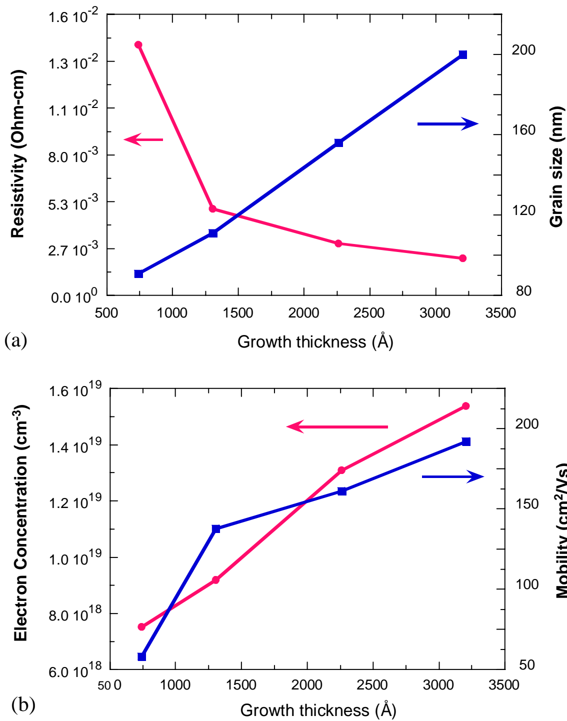

Fig. 5. Dependence of poly-InAs sample (a) resistivity and grain size, and (b) electron concentration and mobility on thickness.

the rapid decrease in resistivity between the 730 and 1300 Å samples is attributed in most part to the sharp increase in mobility between these two samples. This is an interesting observation as the polycrystalline grain size is shown to be somewhat linear in Fig. 5(a).

Size, density, and arrangement of the crystallites may contribute to the nonlinear mobility at lower film thickness. Although the grain size follows a nearly linear relation to growth thickness, it can be seen in Fig. 6 that the thickness dependence of density and arrangement of the crystallites is more complicated. At the smallest thickness, Fig. 6(a), the grain size is larger than the film thickness, and there are voids between the grains. Based on the plan-view SEM images, we suspect that these films may be non-continuous. At the higher depositions, Fig. 6(b)–(d), the grain size is smaller than the film thickness resulting in continuous films. Hall mobility and carrier density measurements cannot be well applied to a non-continuous film, and a non-continuous film would account for the observed variations at lower film thickness.

Cross-sectional SEM images were used to examine the continuity of the poly-InAs at the various growth thicknesses. It was observed that

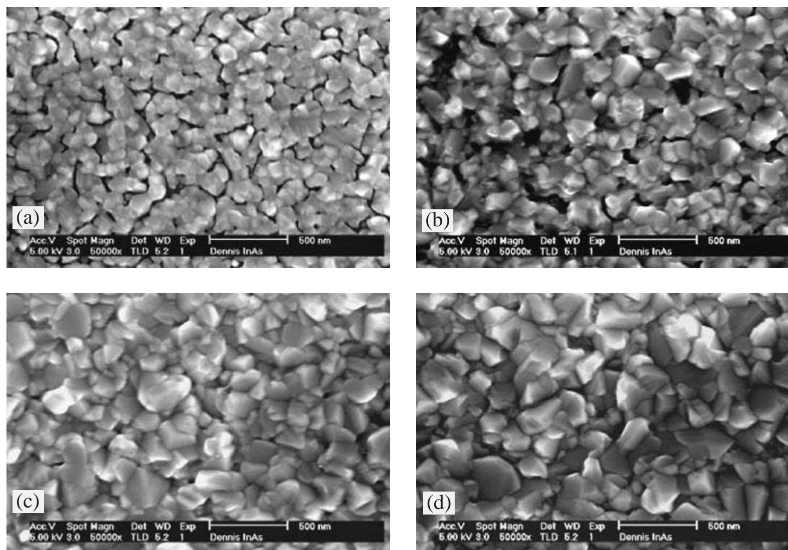

Fig. 6. Plan-view SEM images of poly-InAs samples thicknesses of (a) 730 Å, (b) 1300 Å, (c) 2250 Å, and (d) 3200 Å.

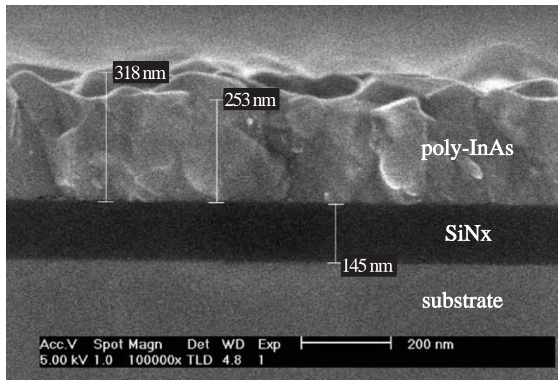

Fig. 7. Cross-sectional SEM image of the 3200 Å poly-InAs sample showing variation in thickness.

the thickness measurements determined by step profilometry are representative only of the *maximum* film thickness. The difference between the minimum and maximum thickness is at least 500 Å in all of the samples. A cross-section of the 3200 Å film is shown in Fig. 7. Measurements show the highest and lowest points of the film as well as the thickness of the underlying SiN_x layer. The 500 Å deviation from maximum film thickness is most apparent in the Hall data for the 730 Å sample, and the effect of the variation becomes less significant as the thickness increases.

The lowest resistivity poly-InAs shown in this work is $2.1 \times 10^{-3}\,\Omega\,\mathrm{cm}$ (Fig. 5(a)). This resistivity is one order of magnitude higher than what is typically expected of the InGaAs emitter capping layer in a conventional InP-based mesa HBT. The proposed structure shown in Fig. 1 does benefit from a larger emitter contact area when compared to the mesa HBT structure. However, further work is warranted to improve the conductive properties of the poly-InAs if it is to be used as an extrinsic emitter contact in a regrown emitter HBT.

4. Conclusion

In this report, we detail the growth and electrical properties of silicon-doped poly-InAs by MBE deposition. We find that poly-InAs is a low-resistance bulk material and that the low contact resistance of monocrystalline InAs is preserved in the polycrystalline material. The resistivity of poly-InAs is found to have a strong dependence on the physical properties of the deposited film, and we report the dependence of these properties with variation in growth temperature, V–III ratio, and deposition thickness. The low-resistivity poly-InAs material is proposed as an extrinsic emitter contact in III–V HBTs similar to the polycrystalline silicon used as contacts in silicon bipolar junction transistor technology.

Acknowledgements

The authors wish to express their gratitude to Dr. Bobby Brar of Rockwell Scientific Company for his helpful and enlightening discussion. This work was supported by the ONR THz Bandwidth Program under contract number N0014-99-1-0041 and the DARPA TFAST Program under contract number N66001-02-C-8080 (UCSB subcontract to Rockwell Scientific Company).

References

[1] T. Nakamura, T. Miyazaki, S. Takahashi, T. Kure, T. Okabe, M. Nagata, IEEE Trans. Electron Devices ED-29 (1982) 596.
[2] M. Takagi, K. Nakayama, C. Terada, H. Kamioka, J. Jpn. Soc. Appl. Phys. 42 (Suppl.) (1973) 101.
[3] K. Washio, in: M. Rodwell (Ed.), International Journal of High Speed Electronics and Systems, World Scientific, Singapore, 2001, p. 77.
[4] S.J. Jeng, B. Jagannathan, J.-S. Rieh, J. Johnson, K.T. Schonenberg, D. Greenberg, A. Stricker, H. Chen, M. Khater, D. Ahlgren, G. Freeman, K. Stein, S. Subbanna, IEEE Electron Device Lett. 22 (2001) 542.
[5] B. Jagannathan, M. Khater, F. Pagette, J.-S. Rieh, D. Angell, H. Chen, J. Florkey, F. Golan, D.R. Greenberg, R. Groves, S.J. Jeng, J. Johnson, E. Mengistu, K.T. Schonenberg, C.M. Schnabel, P. Smith, A. Stricker, D. Ahlgren, G. Freeman, K. Stein, S. Subbanna, IEEE Electron Device Lett. 23 (2002) 258.
[6] J.-S. Rieh, B. Jagannathan, H. Chen, K.T. Schonenberg, D. Angell, A. Chinthakindi, J. Florkey, F. Golan, D. Greenberg, S.J. Jeng, M. Khater, F. Pagette, C. Schnabel, P. Smith, A. Stricker, K. Vaed, R. Volant, D. Ahlgren, G. Freeman, K. Stein, S. Subbanna, IEDM Tech. Dig. (2002) 771.

[7] K. Washio, E. Ohue, R. Hayami, A. Kodama, H. Shimamoto, M. Miura, K. Oda, I. Suzumura, T. Tominari, T. Hashimoto, IEDM Tech. Dig. (2002) 767.
[8] D. Scott, H. Xing, S. Krishnan, M. Urteaga, N. Parthasarathy, M. Rodwell, Device Res. Conf. Tech. Dig. (2002) 171.
[9] Y. Wei, D. Scott, Y. Dong, A.C. Gossard, M.J.W. Rodwell, IEEE Electron Device Lett. (2004) accepted for publication.
[10] S.L. Fu, S.H. Park, Y.M. Hsin, M.C. Ho, T.P. Chin, P.L. Yu, C.W. Tu, P.M. Asbeck, Device Res. Conf. Tech. Dig. (1994) 91.
[11] S.H. Park, T.P. Chin, Q.Z. Liu, S.L. Fu, T. Nakamura, P.K.L. Yu, P.M. Asbeck, IEEE Electron Device Lett. 19 (1998) 118.
[12] C.A. Mead, W.G. Spitzer, Phys. Rev. Lett. 10 (1963) 471.
[13] C.A. Mead, W.G. Spitzer, Phys. Rev. 134 (1964) A713.
[14] D. Scott, M. Urteaga, N. Parthasarathy, M. Rodwell, Lester Eastman Conf. Tech. Dig. (2002) 207.
[15] W.J. Schaffer, M.D. Lind, S.P. Kowalczyk, R.W. Grant, J. Vac. Sci. Technol. B 1 (1983) 688.
[16] B.R. Hancock, H. Kroemer, J. Appl. Phys. 55 (1984) 4239.